UNIVERSIDADE DE SÃO PAULO

INSTITUTO DE FÍSICA
CAIXA POSTAL 66318
05315-970 SÃO PAULO - SP
BRASIL

PUBLICAÇÕES

IFUSP/P-1248

LYAPUNOV GRAPH FOR 2-PARAMETERS MAP: APPLICATION TO THE CIRCLE MAP

J.C. Bastos de Figueiredo and **C.P. Malta**
Instituto de Física, Universidade de São Paulo

Novembro/1996

Lyapunov graph for 2-parameters map: application to the circle map

J. C. Bastos de Figueiredo and C. P. Malta

Instituto de Física, Universidade de São Paulo
CP 66318, 05315-970 São Paulo, BRASIL

Abstract

In a Lyapunov graph the Lyapunov exponent, λ, is represented by a colour in the parameter space. The colour shade varies from black to white as λ goes from $-\infty$ to 0. All the complex dynamics of the circle map ($\theta_{n+1} = \theta_n + \Omega + (1/2\pi)K\sin(2\pi\theta_n)(\mathrm{mod}\ 1)$), can be obtained by analysing its Lyapunov graph. For $K > 1$ the map develops one maximum and one minimum and may exhibit bistability that corresponds to the intersection of topological structures (stabilty arms) in the Lyapunov graph. In the bistability region, there is a strong sensitivity to the initial condition. Using the fact that each of the coexisting stable solution is associated to one of the extrema of the map, we construct a function that allows to obtain the boundary separating the set of initial conditions converging to one stable solution, from the set of initial conditions converging to the other coexisting stable solution.

1 Introduction

The study of nonlinear systems requires the development of tools, analytical and/or numerical, that provide a simple and precise description of their complex behaviour. Here we use a simple graphical method to analyse the basic properties of two-parameter maps that exhibit a maximum and a minimum for some range of parameters. It is well known the existence of superstable orbits associated to the extrema of the map thus giving rise the property of bistability. In the present work, the dynamics of such maps are studied using the Lyapunov graph in the space of parameters. The Lyapunov exponent measures the rate of separation of trajectories starting at points very close to each other in the phase space, therefore it measures the sensitivity to initial conditions. The Lyapunov graph is obtained by plotting the Lyapunov exponent as function of the parameters of the map. This method has been employed successfully in the case of one-parameter maps (Rössler *et al*,1989; Markus, 1990) and we here extend it to the case of two parameters. The map we have chosen to apply the method of the Lyapunov graph is the circle map with sinusoidal nonlinearity. This map has a very rich and complex dynamics, and has been extensively used to model a great variety of systems in physics, biology, neurology, etc (Arnold, 1965; Guevara & Glass, 1982; Kaneko, 1982,1983; Yeh & Kao, 1983; Shell, Fraser & Kapral, 1983; Kapral & Fraser, 1984; Fraser & Kapral,1984; Jensen, Bak & Bohr, 1984; Bohr, Bak & Jensen, 1984; Gambaudo Glendenning & Tresser, 1984; Glass *et al*, 1984; Bélair & Glass, 1985; Mackey & Tresser, 1986; Westerwelt, Gwinn & Teitsworth, 1987; Glass & Mackey, 1988; Casdagli, 1988; Zeller, Bauer & Martiensen, 1995). We shall also present a very simple method to obtain, with respect to the initial condition, the boundary of the basins of attraction in the regions of bistability. It should be emphasized that the method presented here can be applied to any one-dimensional map depending on two parameters, and having the features described above. In the section 2 we present the circle map briefly. In section 3 we present the Lyapunov graph method from which the dynamics of the map can be obtained. It has been shown (Shell, Fraser & Kapral, 1983) that in the bistable regions, each stable solution being associated either to the maximum or to the minimum of map. In section 4 we introduce a function of the initial condition that allows to obtain the boundary separating the initial conditions that converge to the stable solution associated to the minimum of the map from those converging to the stable solution associated to the maximum of the map. In section 5 we present the conclusion.

2 The circle map

It is possible to show that the dynamics of most systems that exhibit the "frequency locking" phenomenon can be modelled by a circle map (Jensen, Bak & Bohr, 1984; Bohr, Bak & Jensen, 1984). The frequency locking phenomenon is a resonance ocurring in a system of two coupled oscillators or in an oscillator driven by an external periodic force. The resonance occurs whenever a harmonic Pf_1 of one oscillator is close to the harmonic Qf_2 of the other oscillator. When this happens, the frequency of the two oscillators are sinchronized or locked in the rational ratio P/Q. In these systems, the interaction between different resonances may

give rise to chaotic motion. The interaction between resonances is caused by the nonlinear coupling (Jensen, Bak & Bohr, 1984).

We shall study the circle map with a sinusoidal nonlinearity,

$$\theta_{n+1} = f(\theta_n) = \theta_n + \Omega + \frac{K}{2\pi}\sin(2\pi\,\theta_n) \bmod 1. \tag{1}$$

It is a map of the circle on itself, with the parametrization $0 \leq \theta_n < 1$. The variable θ_n represents the phase of the oscillating system and is measured in discrete time intervals. The sine term corresponds to a periodic external force with amplitude K, and Ω is the frequency of the system in the absence of the nonlinear term.

The dynamics of the map (1) is partially described by the rotation number, ρ, defined by (Bélair & Glass, 1985; Glass & Mackey, 1988)

$$\rho = \lim_{n\to\infty} \frac{f^n(\theta_0) - \theta_0}{n} \tag{2}$$

where $f^n(\theta_0)$ denotes the nth iteration of θ_0.

In the case of monotonic maps, the limit exists and ρ is independent of θ_0. If the map is not monotonic (its inverse does not exist and it is not a homeomorphism) the limit is of the supreme and ρ will depend on θ_0 (Bélair & Glass, 1985; Glass & Mackey, 1988). For $K < 1$ the map (1) is strictly monotonic (therefore does not depend on θ_0). If $K = 1$ the map (1) develops a cubic inflexion at $\theta = 0$ but it is still invertible. For $K > 1$ the map (1) develops a local minimum and a local maximum, therefore, it cannot be inverted, and, as is well known, chaotic behaviour can occur in this case.

The periodic orbits of the map (1) have rational rotation number ρ; the so called quasi-periodic orbit have irrational rotation number ρ. It has been shown (Arnold, 1965) that for the map (1), for a certain value of Ω, if $0 < K < 1$, the rotation number ρ may take rational values that remain fixed (frequency or phase locking) within certain intervals or windows $\Delta\Omega$. For $K \sim 0$ these intervals are very small so that the probabitity that a random choice of Ω will result in a rational ρ is practically zero. Thus, the probability of ρ being irrational is almost 1, and this means that, for $K \sim 0$, there will be only quasiperiodic orbits. As K is increased, the intervals of frequency-locking increase, and, correspondingly, increases the probability of ρ being rational. For $K \sim 1$, the probability that ρ is rational is almost 1.

The regions of the (Ω, K) space where ρ is rational (resonance windows) are known as the Arnold tongues (figure 1). The resonance windows are separated by quasiperiodic orbits. The width of these resonance windows increases with K so that at $K = 1$ the quasiperiodic orbits constitute a Cantor set of measure zero (Jensen, Bak & Bohr, 1984). The line $K = 1$ on the plane (Ω, K) is called the critical line. Beyond the critical line there is an overlap of resonances that will lead eventually to chaotic motion. When there is an overlap of resonances, the orbit may jump erratically between the different overlapping resonances.

3 The Lyapunov graph method

The quantity

$$\mu = \frac{df^n(\theta)}{d\theta}\,|_{\theta=\theta_i^*} = \prod_{i=0}^{n-1}\left(\frac{df(\theta)}{d\theta}\right)|_{\theta=\theta_i^*} \tag{3}$$

determines the stability of the periodic orbit $\theta_0^*, \theta_1^*, \ldots, \theta_{n-1}^*$ (fixed points). The orbit will be stable (unstable) if $|\mu| < 1$ ($|\mu| > 1$). The case $|\mu| = 1$ is undetermined. The case $(\frac{df}{d\theta}) = 0$ corresponds to the superstable orbit.

For one-dimensional maps, the Lyapunov exponent is defined by

$$\lambda = \lim_{N\to\infty} \frac{1}{N}\sum_{i=0}^{N-1} \ln\left|\frac{df(\theta)}{d\theta}\,|_{\theta=\theta_i}\right|. \tag{4}$$

The Lyapunov exponent measures the rate of separation of different orbits. If $\lambda < 0$ the orbit is stable. The orbit is superstable ($\mu = 0$) if $\lambda \to -\infty$. If $\lambda > 0$ the orbit is unstable and exhibits sensitivity to initial conditions (exponential separation of orbits that are initially very close to each other) (Thompson & Stewart, 1986; Glass & Mackey, 1988).

In order to describe the dynamics of the map (1) we shall graph the Lyapunov exponent λ in the parameter space (Ω, K). As mentioned in the introduction, this technique has been used in the case of a single parameter (the logistic map) by Rössler *et al* (1989), and Markus (1990), and we shall extend it to the case of two parameters.

The Lyapunov graphs are constructed by computing numerically the Lyapunov exponent. Starting from an initial condition θ_0, 6000 iterations are performed. The first 1000 iterarions are discarded (in order to eliminate possible transients) and the Lyapunov exponent (4) is calculated using the other 5000 iterations. The graphs have been computed for $0 \leq \Omega \leq 1$ and $0 \leq K \leq \pi$.

The value of θ_0 may be kept fixed at a value chosen arbitrarily or it may be chosen randomly ($0 \leq \theta \leq 1$) so as to investigate the effects of initial condition fluctuations upon the stability of the system.

The figure 2 displays the Lyapunov graph obtained using the initial condition $\theta_0 = 0.50$. The lighter the colour, the less negative is the exponent. The white regions correspond to quasiperiodic orbits and in the regions that are almost white the stability is changing (bifurcation points). The structure known as Arnold tongues (see figure 1) is easily seen in the interval $0 < K < 1$, in which the white colour predominates. Each tongue corresponds to a region of frequency locking with $\rho = P/Q$. The tongues width increases with K and they do not overlap for K in that interval (they are separated by white regions corresponding to quasiperiodic orbits). As already mentioned, for $K \sim 0$ the orbits are quasiperiodic so the tongues are not visible in this situation (white region). Beyond the critical line ($K = 1$) a drastic change in the topology of the graph is observed, the black colour predominating for $K > 1$. For $K > 1$ the map (1) is not monotonic and there is an overlap of resonances

that eventually leads to chaotic dynamics. Beyond the critical line, there exists a complex bistability structure.

The Lyapunov graph displayed in the figure 2–a exhibits a very important property: self-similarity. This self-similarity is evident below the critical line. Above the critical line, the self-similarity is illustrated by the zoom displayed in figure 2–b, thus indicating that scaling laws must also exist above the critical line (as predicted in Shell, Fraser & Kapral, 1983).

The curves corresponding to the superstable orbits can be seen above the critical line. Generically, inside each region characterized by $\rho = P/Q$, there will be a main superstable curve, tangent to the critical line $K = 0$, associated to superstable orbits of period Q. On the main superstable curve the map has an inflexion. The superstable curves are related by a period-doubling cascade corresponding to the period-doubling cascade exhibited by the superstable orbits. In figure 3, we can see the superstable curves (in black) inside the tongue with $\rho = 0$. The main superstable curve, tangent to the critical line, has period 1. Above it, there is a pair of intersecting superstable curves of period 2 and further above there are two pairs of intersecting superstable curves of period 4, and so on. Each pair of superstable curves intersect each other twice, forming a loop. One of the intersections corresponds to a doubly stable orbit (the minimum of the map (1) is mapped onto the maximum and vice-versa), and the other one corresponds to the coexistence of two superstable orbits (bistability), one of them associated to the maximum of the map (1) and the other one to its minimum. This is a *local bistability* (Shell, Fraser & Kapral, 1983) as it envolves only local structures within the same frequency-locking region.

In the figure 2 we can see that, above the critical line, the tongues develop pairs of stable arms, one going up towads the left and the other one towards the right. As K increases, the width of the arms decreases, and for large values of K the arms belonging to different tongues tend to align parallel to each other with slopes equal to $\pm 2\pi$. The external boundary of the arm is a continuation of the boundary of the tongue. It is determined by the points where a stable periodic orbit appears as a result of a tangent bifurcation, its period being equal to the fundamental period of the tongue. For a tongue of fundamental period n, the external boundary is obtained by solving the following equations:

$$f^n(\theta) = 0 \,, \tag{5}$$

$$\frac{df^n}{d\theta}(\theta) = 1 \,. \tag{6}$$

Moving across the arm, there will be a period doubling cascade after which an attractor will be generated. The internal boundary of the arm is determined by the points where the attractor loses stability via a boundary crisis, as discussed by Grebogi, Ott & York (1982, 1983). Due to the auto-similarity property this structure is repeated *ad infinitum* inside an arm (Kapral and Fraser, 1984)(see figures 2–a,b). Figures 2 and 3 show that each arm encloses a sequence of superstable curves. The arms going up towards left (right) enclose the superstable curves associated to the maximum (minimum) of the map. The intersection of arms, corresponding to different frequency-locking values, gives rise to the *nonlocal bistability*. Like in the case of local bistability, one of the coexisting stable solutions

is associated to the maximum of the map (it belongs to the arm that encloses superstable curves associated to the maximum of the map) and the other one to its minimum (it belongs to the arm that encloses superstable curves associated to the minimum of the map). The fact that each stable solution can be associated to the maximum or the minimum of the map will allow us to obtain the boundary separating the set of initial conditions converging to one stable state, from the set converging to the other coexisting stable state.

Figure 4 shows the intersection of the left (right) arm of the central tongue, for which $\rho = 1/2$, and the right (left) arm of the tongue with $\rho = 1/3$ ($\rho = 2/3$). The Lyapunov graph in figure 4–a was obtained starting at $\theta_0 = 0.1$ and we notice that in the intersection region there seems to be a preference for one of the arms, depending on the parameters value, resulting in an approximate symmetry with respect to $\Omega = 0.5$. However, this symmetry is recovered by using initial condition θ_0 randomly chosen in the interval $[0, 1]$, as exhibited in Figure 4–b. Therefore, at these intersections, there coexist two stable solutions that are strongly sensitive to the initial condition θ_0. Two initial conditions, that are very close, may converge to different arms. Also, the same initial condition, for slightly different parameters in the intersection region will, in general, converge to different states. Nevertheless, we shall show that, given an initial condition θ_0, if the mapping is associated to the minimum (maximum) of the map, it will converge to the arm going up towards right (left). Due to this, we shall denote by m (M) the arm going up towards right (left).

In Figure 5 we display the Lyapunov graph showing the intersection of the arm m of the tongue with $\rho = 0$, and the arm M of the tongue with $\rho = 1$. The external boundaries of the arms, as already mentioned, are determined by tangent bifurcations. So, they are obtained by solving the following system of equations (see equations (1) and (6))

$$\theta + \Omega + \frac{K}{2\pi}\sin(2\pi\,\theta) = \theta \,, 1 + K\cos(2\pi\,\theta) = 1 \,. \tag{7}$$

The solutions of the above system are $K = \pm 2\pi\,\Omega$, confirming our assertion that, above the critical line, all the tongues have the arms aligned in the directions $\pm 2\pi$.

The points of maximum and mimimum of the map (1) are provided by the equation

$$\frac{df(\theta)}{d\theta} = 1 + K\cos(2\pi\,\theta) = 0 \,, \tag{8}$$

which solutions are given by $\theta_{\max} = \frac{1}{2\pi}\arccos(-\frac{1}{K})$ and $\theta_{\min} = -\frac{1}{2\pi}\arccos(-\frac{1}{K})$. These solutions will exist only for $|K| \geq 1$, in agreement with the monotonicity condition, $|K| < 1$. The maps of $\theta_{\max}$ and $\theta_{\min}$, along the external boundary of m (M) are obtained by using $K = 2\pi\,\Omega$ ($K = -2\pi\,\Omega$) in equation (1). The result for m is

$$f_{m,\min}(\Omega) = \Omega - \frac{1}{2\pi}\arccos(-\frac{1}{2\pi\,\Omega}) + \Omega\sin\left[-\arccos(-\frac{1}{2\pi\,\Omega})\right] \,, \tag{9}$$

$$f_{m,\max}(\Omega) = \Omega + \frac{1}{2\pi}\arccos(-\frac{1}{2\pi\,\Omega}) + \Omega\sin\left[\arccos(-\frac{1}{2\pi\,\Omega})\right] \,, \tag{10}$$

and for M is

$$f_{M,\min}(\Omega) = \Omega - \frac{1}{2\pi}\arccos(\frac{1}{2\pi\,\Omega}) - \Omega\sin\left[-\arccos(\frac{1}{2\pi\,\Omega})\right] , \quad (11)$$

$$f_{M,\max}(\Omega) = \Omega + \frac{1}{2\pi}\arccos(\frac{1}{2\pi\,\Omega}) - \Omega\sin\left[\arccos(\frac{1}{2\pi\,\Omega})\right] . \quad (12)$$

The above functions are displayed in the figure 6. As we can see, $f_{m,\min}(\Omega)$ ($f_{M,\max}(\Omega)$) tends very fast to a constant value while $f_{m,\max}(\Omega)$ ($f_{M,\min}(\Omega)$), as we have removed the mod 1, increases approximately linearly (taking into account the mod 1 we would obtain a sawtooth function). This behaviour explains why the Lyapunov graph reproduces so well the dynamics of the map (1). All the points belonging to the external boundary of the arm m (M) will have Lyapunov exponents (3) that are very close because $f_{m,\min}(\Omega)$ ($f_{M,\max}(\Omega)$) varies very little for $\Omega \geq 0.5$. At the intersection of the arm m of any tongue, and the arm M of another tongue, the points belonging to the arm M are distinguished from the points belonging to the arm m because they will have completely different Lyapunov exponents.

In order to better illustrate how precise the Lyapunov graph is in describing the dynamics of a map, we have calculated the bifurcation diagram as one moves along the external boundary $K = 2\pi\,\Omega$ of the arm m of the tongue with $\rho = 0$ (see figure 5). In the figure 7 we display this bifurcation diagram, for 1000 values of Ω uniformly distributed in the interval $[0.45, 0.65]$, starting from values of θ_0 in the interval $[0, 1]$, and iterated 4000 times. At $\Omega = 0.50$, the external boundary $K = 2\pi\,\Omega$ of the arm m of the tongue with $\rho = 0$ (see figure 5) intersects the external boundary $K = -2\pi\,\Omega$ of the arm M of the tongue with $\rho = 1$, indicating bistability. Indeed, this bistability is seen in the figure 7, in which two stable states (and one unstable) coexist for Ω in the interval $[0.50, 0.55]$. In the interval $[0.55, 0.62]$ the bifurcation diagram (figure 7) shows the coexistence of a stable state with a period-doubling sequence that culminates in an attractor that is destroyed, via a boundary crisis (Grebogi, Ott & York, 1982,1983), at $\Omega = 0.62$. In this interval, figure 5 shows that the boundary $K = 2\pi\,\Omega$ crosses the interior of the arm M, therefore crossing the superstable curves that belong to a period doubling sequence that culminates in an attractor. At $\Omega = 0.62$, the external boundary $K = 2\pi\,\Omega$ crosses the internal boundary of the arm M of the tongue with $\rho = 1$, so, only the state belonging to the arm m will exist in the rest of the interval considered, the same being true of the bifurcation diagram in figure 7.

4 Boundary of the basins of attraction of initial conditions

As already mentioned, the superstable curves associated to the minimum (maximum) of the map (1) belong to m (M). The fact that the mapping of the minimum inside m, $f_{m,\min}(\Omega)$ (figure 6–b), varies very little (in particular, it is approximately constant in the region of intersection of arms m and M) the same being true of the mapping of the maximum inside M, $f_{M,\max}(\Omega)$ (figure 6–c), indicates that the stable solutions belonging to an arm m have a point that remains closer to the minimum of the map while the stable solutions belonging to an arm M have a point that remains closer to the maximum of the map. This is illustrated in

the figures 8–a,b where we display two orbits of period-4, and a chaotic attractor, respectively. The orbit (solid line), having one of its points closer to the maximum of the map, belongs to the arm M of the tongue with $\rho = 1$, and the orbit (dashed line), having one of its points closer to the minimum of the map, belongs to the arm m of the tongue with $\rho = 0$; the chaotic attractor in the figure 8-b belongs to the arm M and it is clearly seen that it is closer to the maximum of the map. Therefore we can say that the dynamics of an arm m (M) is determined by the minimum (maximum) of the map (1).

As we have seen, for (K, Ω) in the regions of intersection of arms m and M, given an initial condition θ_0, its iteration may converge to the stable state belonging to one arm or the other. By using the fact that the dynamics of the arms is determined by the closeness of the iterations of θ_0 to the maximum or the minimum of the map (1), we can obtain the boundary separating the set of initial conditions converging to the stability arm m, from the set of initial conditions converging to the stability arm M. As the iteration of θ_0 approaches an extremum, $\frac{df(\theta)}{d\theta} = f'(\theta) \to 0$, with $f''(\theta) > 0$ in the case of a minimum, and $f''(\theta) < 0$ in the case of maximum. The figure 9 shows the map $f(\theta)$ (1) (without mod 1, for simplicity), and the function $\frac{f''(\theta)}{|f'(\theta)|}$. As we can see, in the vicinity of the maximum (minimum) of f the function $\frac{f''(\theta)}{|f'(\theta)|}$ diverges towards $-\infty$ ($+\infty$). Therefore, in order to determine to which extremum an orbit is closer, for N consecutive iterations of some initial condition θ_0, we compute the value of the following average

$$\Delta = \lim_{N\to\infty} \frac{1}{N} \sum_{i=0}^{N-1} \frac{f''(\theta_i)}{|f'(\theta_i)|} . \quad (13)$$

In general, the points θ_i lying distant from the extrema will give a small contribution to Δ because $\frac{f''(\theta)}{|f'(\theta)|}$ is small and, moreover, the contribution due to points on the monotonic branch of the map to the left of the maximum has the opposite sign of the contribution due to points on the monotonic branch of the map to the right of the minimum of the map. Therefore, the value of Δ is determined by the points θ_i lying closer to the extrema, thus, given θ_0, if $\Delta > 0$ ($\Delta < 0$) the orbit is closer to the minimum (maximum), consequently, the solution will belong to an arm m (M). So, for any point of the parameter space (Ω, K), given an initial condition θ_0, we can determine whether the solution will belong to an arm m or to an arm M. To illustrate this method, we have calculated Δ on the line $K = 1.65$ in the figure 4–a, using 750 initial conditions θ_0 in the interval $[0, 1]$, and 750 values of Ω, uniformly distributed in the interval $[0.40, 060]$. Each θ_0) was iterated 4000 times, the initial 1000 iterations were discarded, and the results are exhibited in the figure 10, the points (Ω, θ_0) corresponding to $\Delta < 0$ being plotted in black and the points corresponding to $\Delta > 0$ being plotted in white. For $0.4 \leq \Omega < 0.408$, the plot $\theta_0 \times \Omega$ shows a white stripe with scattered black dots. Examining the figure 4–a, we notice that this interval precedes the point where the line $K = 1.65$ starts crossing the arm M of the tongue $\rho = 1/2$; this region contains many intersections of arms M and m (see Figure 2–a), so, the white areas corresponds to arms of type m and the black dots to arms of type M. At $\Omega = 0.408$, the line $K = 1.65$ crosses the external boundary of the arm M of the tongue $\rho = 1/2$, and remains inside M until $\Omega = 0.411$. So, in the interval $[0.408, 0.411]$, the dynamics is associated to the maximum, thus the corresponding thin black stripe in the graph $\theta_0 \times \Omega$ (see figure 10). In the interval

$0.411 < \Omega < 0.426$ there is bistability (see figure 4-a), due to the intersection of the arm M with the arm m of the tongue with $\rho = 1/3$. Correspondingly, the graph $\theta_0 \times \Omega$ exhibits an area in which white and black areas are separated by regions of uniformly distributed black and white dots so that, depending on the initial condition, the system will converge to a state belonging to m or to M. We have numerically verified that the initial condition boundary is fractal in this interval. The white spots appearing in the neighbourhood of $\Omega = 0.45$ corresponds to the intersection with the arm m (the string of black dots crossing M in the figure 4–a) of the tongue with $\rho = 2/5$. As already mentioned, the superstable curves intersect twice, forming a loop. In the neighbourhood of the superstable curves, the dynamics is determined by them. Thus the two stripes, white and black, that are seen to the left and right, respectively, of $\Omega = 0.50$, which is the point where the period-4 superstable curves intersect each other. After crossing the region of intersection of the superstable curves, the line $K = 1.65$ enters the arm m of the tongue $\rho = 1/2$ (see figure 4–a), resulting in the wide white stripe seen in the graph $\theta_0 \times \Omega$. The black spots seen in the vicinity of $\Omega = 0.55$ are due to intersection of the arm M (string 0f black dots seen crossing the arm m in the figure 4–a) of the tongue with $\rho = 3/5$. The fractal boundary in the interval $[0.574, 0.589]$ corresponds to the bistability region resulting from the intersection with the arm M of the tongue with $\rho = 2/3$. In fact, this fractal stripe can be obtained from the previous fractal stripe by exchanging black and white, and then making the transformation $\theta_0 \rightarrow (1 - \theta_0)$. So, our results have shown that the evaluation of the Δ (equation (13)) provides a way of separating the set of initial conditions converging to an arm m (dynamics associated to the minimum of the map), from the set of initial conditions converging to an arm M (dynamics associated to the maximum of the map).

5 Conclusion

We have extended the method of Lyapunov graph to the case of 2-parameters map. Applying this method to the case of the circle map, we have shown that the Lyapunov graph exhibits all the complexities of map dynamics. It reproduces the Arnold tongues below the critical line $K = 1$, and, above the critical line it reproduces the superstable curves, the bistability regions and the self-similarity structure characteristic of the circle map. The Lyapunov graph also exhibits the strong sensitivity to the initial condition in the bistability region.

Above the critical line (when the map is non-monotonic), the continuation of the Arnold tongues develop two arms. We have shown that the left arm (M) is associated to the maximum of the map, and the right arm (m) is associated to the minimum of the map. Using this fact, we have constructed the function *Delta* (equation (13)) that, for a given initial condition, indicates to which of the coexisting stable solutions it will converge. Bistability occurs at the intersection of arms M and m belonging to different tongues. If $\Delta < 0$ the initial condition will converge to the stable solution belonging to the arm M and if $\Delta > 0$ it will converge to the stable solution belonging to the arm m. The plot of $\theta_0 \times \Omega$ (figure 10) provides the boundary separating the set of initial conditions converging to the arm m, from the set of initial conditions converging to the arm M. The figure 10 was obtained by iterating 4000 each initial condition, the initial 1000 iterations being discarded, but it

should be remarked that, when the solution is periodic, after the transient of 1000 iterations, a number of iterations equal to a period is enough to calculate Δ.

This method of the Lyapunov graph can be applied to any 2-parameters map. The function Δ can also be used for determining the boundary of the basin of attraction of initial condition, provided the map has one of the stable solutions with dynamics associated to the minimum of the map and the other one associated to the maximum of the map. moreover, this method can be used to investigate the effect of addition of noise to the map.

Acknowledgemet

JCBF is financially supported by CNPq (Brazilian National Council) and CPM acknowledges partial financial support by CNPq.

6 References

Arnold, V. I. ,1965 *Am. Math. Soc. Trans.* **46**, 213–284.

Bélair, J. & Glass, L., 1985 *Physica D* **16**, 143–154.

Bohr, T., Bak P., & Jensen, M. H., 1984 *Phys Rev A* **30**, 1970–1981.

Casdagli, M., 1988 *Physica D* **29**, 365–386.

Fraser R. & Kapral, J., 1984 *Phys. Rev. A* **30**, 1017–1025.

Gambaudo, J. M., Glendinning, P. & Tresser, C., 1984 *Phys Lett A* **105**, 97–100.

Glass, L., Guevara, M. R., Bélair, J. & Shrier, A., 1984 *Phys Rev A* **29**, 1348–1357.

Glass, L. & Mackey, M. C., 1988 *"From Clocks to Chaos: the rythms of life"*, Princeton University Press, New Jersey.

Grebogi,C., Ott, E. & York, J. A., 1982 *Phys. Rev Lett.* **48**, 1507–1510.

Grebogi,C., Ott, E. & York, J. A., 1983 *Physica D* **7**, 181–200.

Guevara, M. R. & Glass, L., 1982 *J. Math. Biol.* **14**, 1–23.

Jensen, M. H., Bak, P. & Bohr, T., 1984 *Phys. Rev A* **30**, 1960–1969.

Kaneko, K., 1982 *Prog. Theor. Phys.* **68**, 669–672.

Kaneko, K., 1983 *Prog. Theor. Phys.* **69**, 403–414.

Kapral, R. & Fraser, S., 1984 *J. Chem. Phys* **88**, 4845–4855.

Mackey, M. C. & Tresser, C.,1986 *Physica D* **19**, 206–237.

Markus, M., 1990 *Computer in Physics* **set/out**, 481–493.

Rössler, J., Kiwi, M., Hess, B. & Markus, M., 1989 *Phys Rev A* **39**, 5954–5960.

Shell, M., Fraser, S. & Kapral, R., 1983 *Phys. Rev. A* **28**, 373–378.

Thompson, J. M. T. & Stewart, H. B., 1986 *Nonlinear Dynamics and Chaos*, John Wiley, Chichester, New York, Brisbane, Toronto & Singapore.

Westerwelt, R. M., Gwinn, E. G. & Teitsworth, S. W., 1987 *Nucl. Phys. B* (Proc Supl) **2**, 37–48.

Yeh,W. J. & Kao, Y., H., 1983 *Appl. Phys. Lett.* **42**, 299–301.

Zeller, M., Bauer, M. & Martienssen, 1995 *Chaos, Solit. & Frac.* **5**, 885–893.

FIGURES AND CAPTIONS

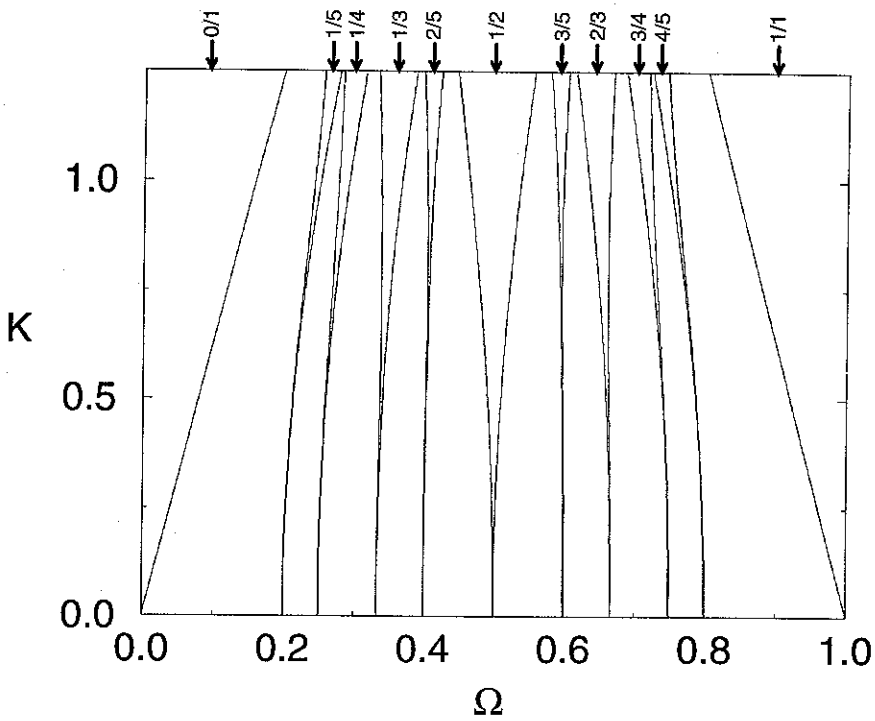

Figure 1: The Arnold tongues boundaries in the parameter space.

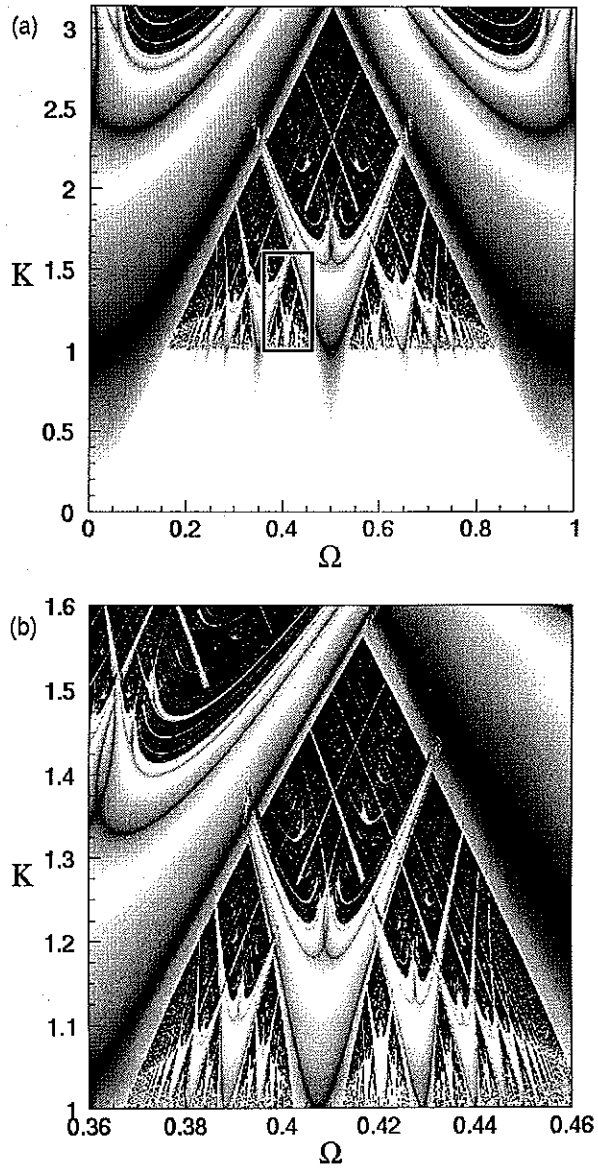

Figure 2: (a) The Lyapunov Graph obtained using $\theta_0 = 0.50$; (b) shows a zoom of the rectangle in the figure (a), illustrating the property of self-similarity.

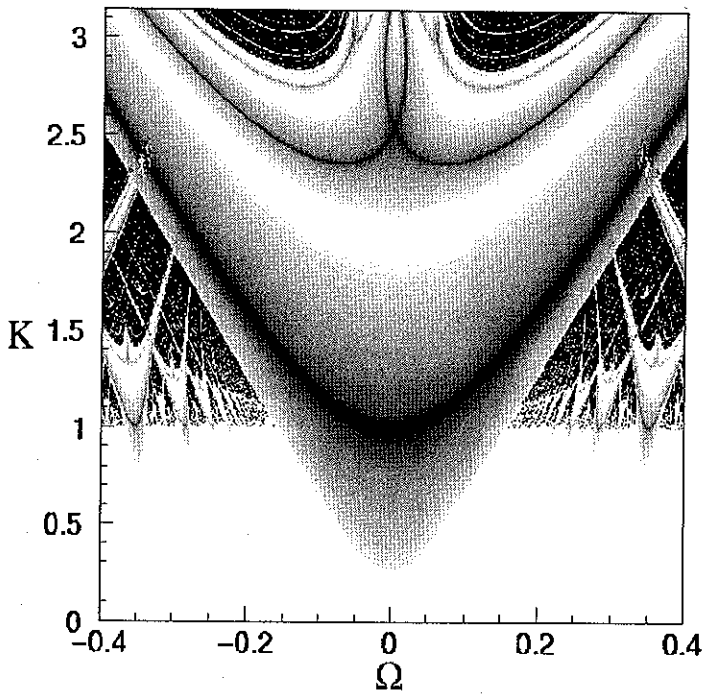

Figure 3: The Lyapunov graph showing the tongue with $\rho = 0$ and its enclosed superstable curves. It has been generated using $\theta_0 = 0.5$.

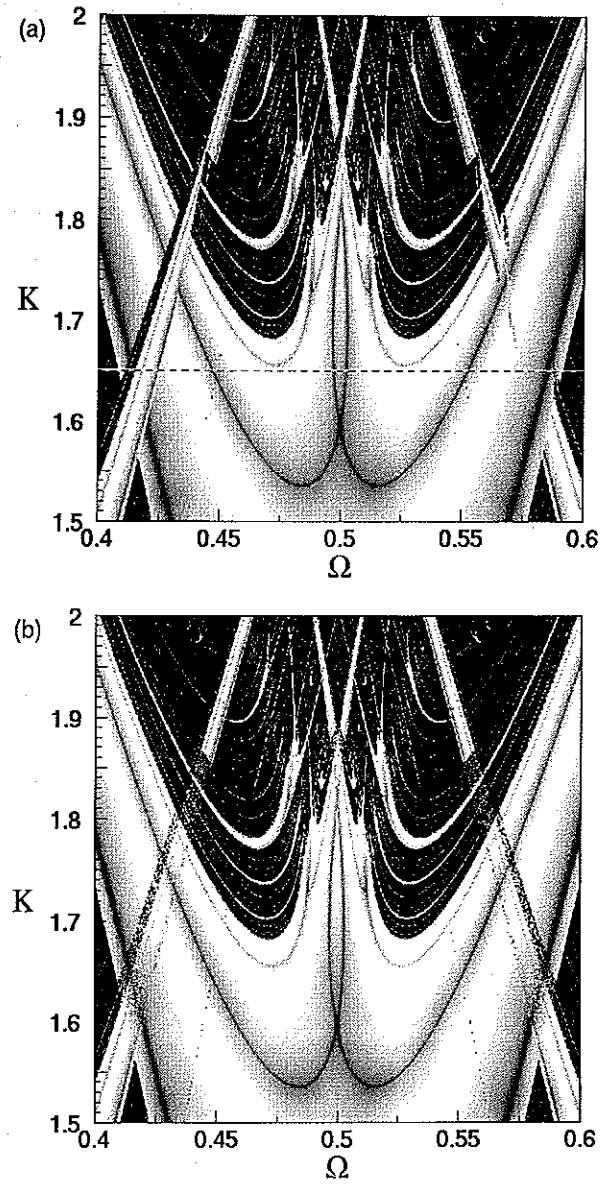

Figure 4: Intersection of the left and right arms of the tongue with $\rho = 1/2$ with the left arm of the tongue with $\rho = 2/3$ and the right arm of the tongue with $\rho = 1/3$, respectively. In (a) the (asymmetric) Lyapunov graph was generated using $\theta_0 = 0.1$ and in (b) the symmetry was obtained by using θ_0 randomly generated in the interval $[0, 1]$. The dashed line in (a) corresponds to the line $K = 1.65$.

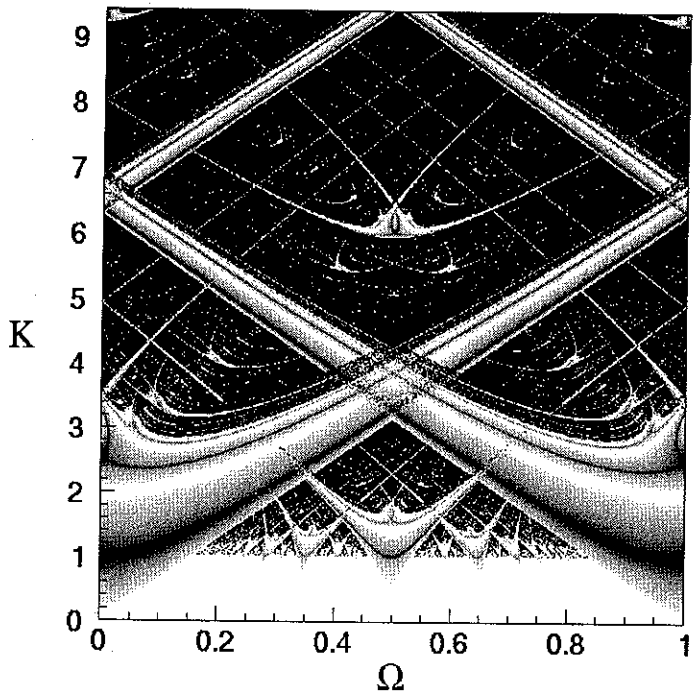

Figure 5: Intersection of the arm m of the tongue with $\rho = 0$ and the arm M of the tongue with $\rho = 1$. This Lyapunov graph was obtained using θ_0 randomly generated in the interval $[0, 1]$.

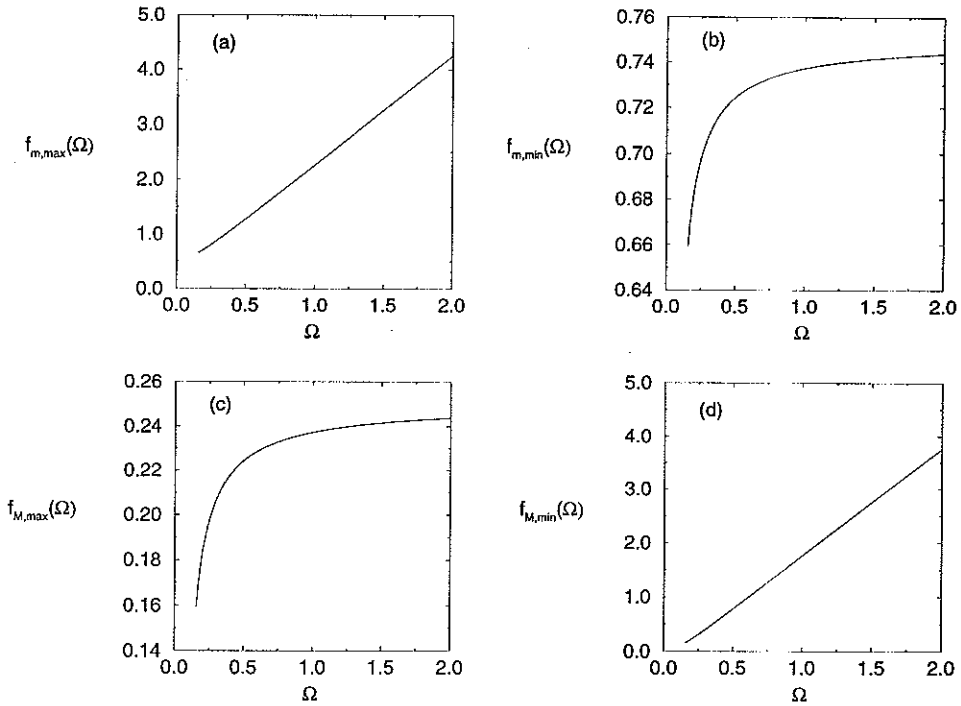

Figure 6: First iterate of the extrema of the map. (a) $f_{m,\max}$, (b) $f_{m,\min}$, (c) $f_{M,\max}$, (d) $f_{M,\min}$.

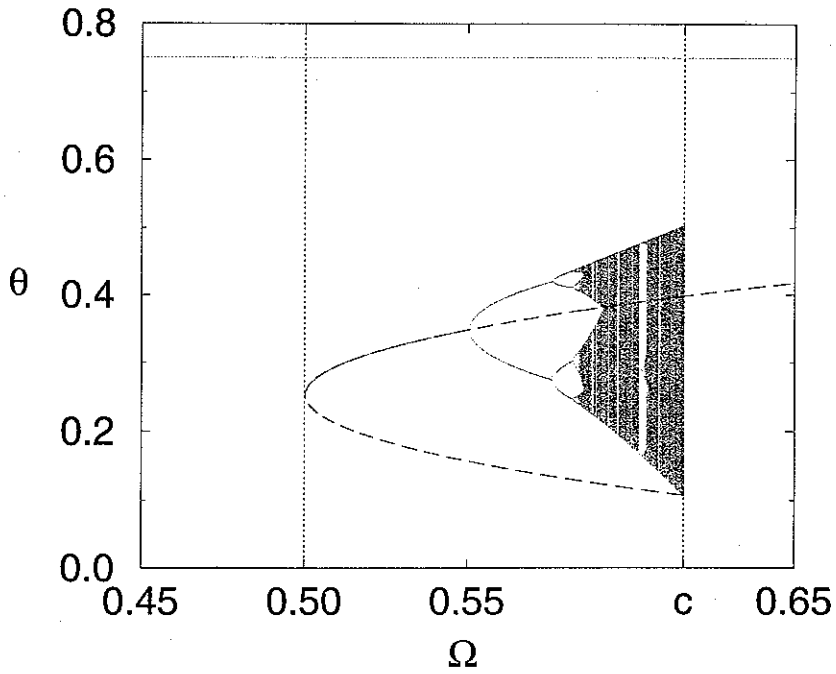

Figure 7: Bifurcation diagram obtained by moving along the boundary $K = 2\pi\Omega$ of the arm m of the tongue with $\rho = 0$. The diagram was obtained by iterating 100 initial conditions θ_0 uniformly distributed in the interval $[0, 1]$. Each initial condition was iterated 4000 times, and the initial 1000 iterations were discarded (transient). The boundary crisis occurs at $c = 0.61625 \approx 0.62$.

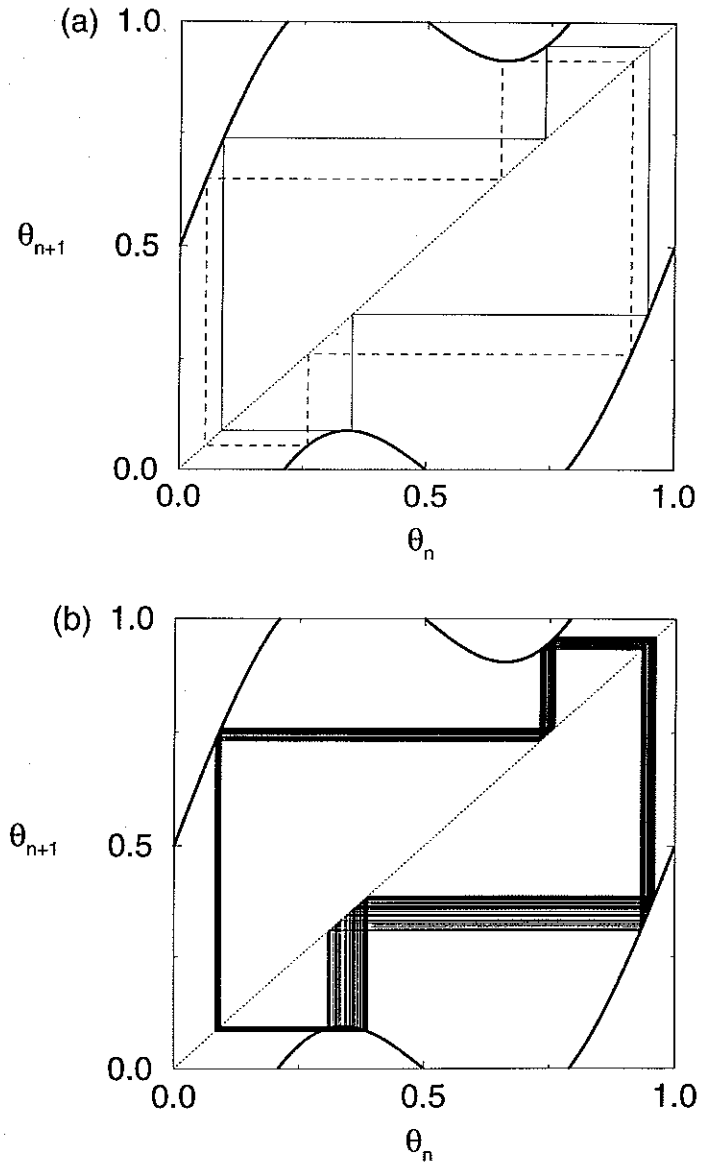

Figure 8: (a) period-4 orbit closer to the maximum (solid line) and period-4 orbit closer to the minimum (dashed line); (b) chaotic attractor closer to the maximum.

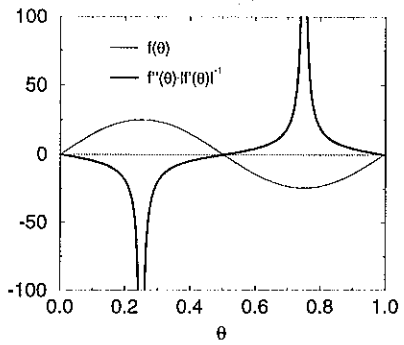

Figure 9: Illustrates the divergence of $f''/|f'|$ at the extrema of the map f (eq (1), without the mod 1). The parameter values are: $\Omega = 0.0, K = 50\pi$.

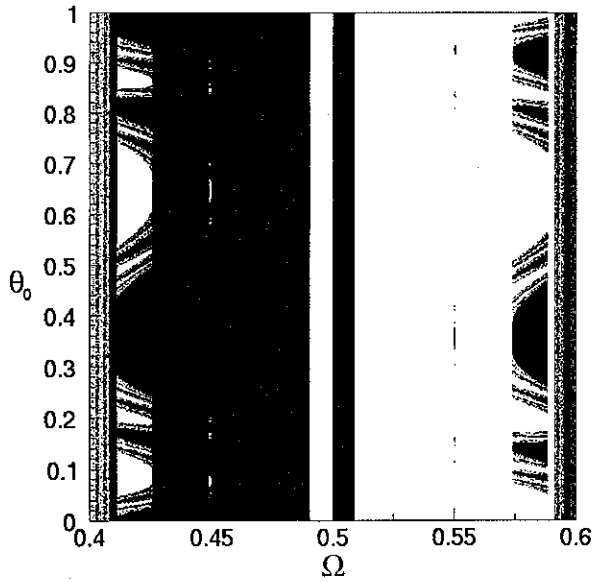

Figure 10: Set of initial conditions converging to the arm m of the tongue $\rho = 0$ ($\Delta > 0$, white points), and set of initial conditions converging to the arm M of the tongue $\rho = 1$ ($\Delta < 0$, black points). It correspond to the dashed line $K = 1.65$ drawn in figure 4-a. We have used 750 values of θ_0 and Ω, uniformily distributed in the corresponding interval. Total number of iterations: 4000; number of iterations discarde (transient):1000.